

A Frequency Invariant Beamformer for Channel Parameter Estimation in Millimeter Wave Bands

Ines Carton, Wei Fan, Gert F. Pedersen

Department of Electronic Systems, Faculty of Engineering and Science, Aalborg University, Aalborg, Denmark

Email: {icl, wfa, gfp}@es.aau.dk

Abstract—Millimeter wave (mm-wave) bands offer vast amounts of unlicensed and unused spectrum that could potentially be utilized by future (5G) wireless systems. Accurate channel characterization at mm-wave bands is required for system design and performance analysis of future 5G communication systems. Knowledge of delay and angle of arrival (AoA) of the incoming multipath components are especially important for future applications at these frequencies. This paper discusses the use of a frequency invariant beamforming (FIB) technique with a uniform circular array (UCA) for the estimation of delay and AoA parameters at mm-wave bands. Simulations are performed for a multipath channel showing the advantages of the discussed frequency invariant techniques compared to traditional beamforming approaches.

Index Terms—Wideband angle estimation, millimeter wave, frequency invariant beamforming, angle-delay estimation.

I. INTRODUCTION

The ever-growing demand for higher data rates in mobile communications has motivated research in millimeter wave (mm-wave) frequency bands for 5G cellular systems. mm-wave bands offer vast amounts of unlicensed and unused spectrum that need to be accurately characterized for the implementation of future 5G communication systems. In addition, mm-wave bands provide as well the possibility of implementing massive array antennas, and better frequency reuse in small cells [1]. In-depth knowledge of the radio channel is important for wireless communication modeling and system design [2]. More specifically, accurate methods to determine the angle and delay of the incoming waves are always desirable. Different ways to estimate angle of arrival (AoA) are investigated in the literature, e.g. high-gain directional antenna, synthetic aperture and beamforming methods, and high resolution algorithms such as MUSIC or ESPRIT [3]. Although extensive studies have been carried out on AoA estimations in the literature, some limitations still exist:

- High-gain directional antenna often suffers from relatively low spatial resolution and embedding of the antenna patterns in the results.
- In practical measurements, the measured channel impulse response (CIR) is essentially only one snapshot of the environment, i.e. only one temporal observation of the channel is available. The spatial methods discussed in [4], e.g. high resolution algorithms like MUSIC cannot directly be applied, as the covariance matrix of the array outputs would be rank-deficient due to the limited

temporal samples. Different algorithms were proposed to address this issue, e.g. obtaining more samples via the spatial smoothing technique in [3] and the iterative 2D Unitary ESPRIT method in [5] for virtual planar arrays.

- Most measurements performed at current cellular bands were narrowband, i.e. the bandwidth is small compared with the carrier frequency [3]. However, this assumption is no longer valid in for mm-wave measurements, where a large bandwidth is often available. The main problem for conventional beamforming in wideband is that the beam pattern is frequency-variant (i.e. the array response is frequency dependent), and hence the results are deteriorated.

Frequency-invariant beamforming (FIB) techniques have been investigated intensively from the signal processing point of view [6]–[9]. In [10], a FIB algorithm was used to estimate the angle and delay of the direct path between the transmitter and receiver for indoor ranging and localization purposes. However, very few papers have utilized FIB techniques for channel parameters estimation. In this paper, a frequency invariant beamforming technique is investigated for estimating the angle and delay of multipath components. The proposed technique can be potentially used for wideband mm-wave channel measurements, e.g. via vector network analyzer (VNA).

In Section II, the conventional beamforming and the FIB techniques for delay and angle estimation using a uniform circular array (UCA) are explained in detail. In Section III, simulation results with the two described methods are shown. Finally, Section IV concludes the paper and discusses the future work.

II. ANGLE ESTIMATION METHOD

In this section we will explain the conventional beamforming and FIB method to estimate the angle of arrival using a UCA based on [10]. A UCA is preferable to a uniform linear array (ULA) because the pattern of the UCA is uniform around the azimuth direction, whereas the ULA's angular resolution is higher at boresight than at endfire direction. Moreover, with a ULA it is not possible to distinguish paths that are symmetric with respect to the array line. Note that the separation between two consecutive elements has to be at most half wavelength for the highest considered frequency in order to avoid spatial aliasing. Note that the following analysis is limited to the azimuth plane, i.e. elevation angle $\theta = \pi/2$.

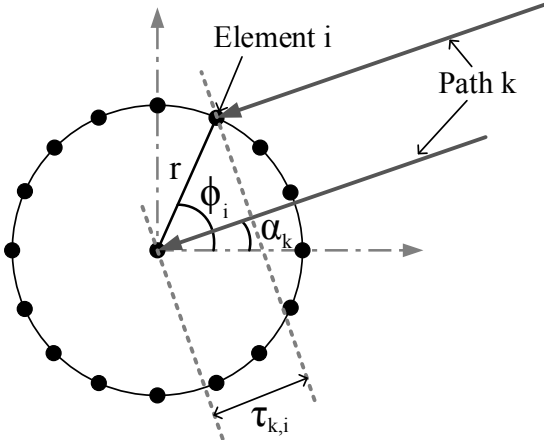


Fig. 1. Multipath component k impinging UCA at angle α_k .

A. Classical Beamforming

A UCA with P array elements placed uniformly around its perimeter of radius r is shown in Fig. 1. Each array element is placed at an azimuth angle $\phi_i = 2\pi i/P$ with $i = 0, \dots, P-1$. The figure shows a multipath component k impinging the UCA from an angle α_k . The frequency response at the center of the UCA is:

$$H(f) = \sum_{k=0}^{K-1} b_k \exp(-j2\pi f \tau_k) \quad (1)$$

where K is the total number of multipath components, b_k and τ_k is the complex amplitude and the delay of the k -th multipath component at the center of the UCA. Assuming that the impinging waves are planar, the delay at the i -th element of the array with respect to the center is:

$$\tau_{k,i} = -\frac{r}{c} \cos(\phi_i - \alpha_k) \quad (2)$$

The frequency response at the i -th element of the UCA is a shifted version of $H(f)$:

$$H_i(f) = \sum_{k=0}^{K-1} b_k \exp(-j2\pi f(\tau_k + \tau_{k,i})) \quad (3)$$

Using classical beamforming, the spatial frequency response can be calculated by shifting the phase of each element's frequency response back to the center of the UCA:

$$H(f, \phi) = \frac{1}{P} \sum_{i=0}^{P-1} H_i(f) \exp(-j2\pi f \frac{r}{c} \cos(\phi + \phi_i)) \quad (4)$$

With this approach, a power peak appears for $\phi = \alpha_k$. By applying the inverse discrete Fourier transform (IDFT) to the previous equation, the spatial channel impulse response can be recovered:

$$h(t, \phi) = \sum_{l=0}^{B/\Delta f} H(f, \phi) \exp(j2\pi ft) \quad (5)$$

where the frequency has been discretized as $f = f_c - (B/2) + l \cdot \Delta f$. The carrier frequency and the bandwidth are f_c and B ,

whereas Δf and l represent the frequency step and the total number of frequency samples, respectively.

The main limitation of conventional beamforming techniques is that the array response is frequency dependent, thus high side lobes appear on the final impulse response as it will be shown in section III. The solution to overcome this is to use FIB techniques.

B. Frequency Invariant Beamforming

The goal of FIB is to find a basis function that converts the frequency dependent array response into a frequency-invariant response [6]. The basis function can be found, for instance, using least-squares solutions, or beam steering [6]. An analytical solution exists for certain array geometries, e.g. UCA [6], [10], uniform concentric circular array (UCCA) [9], or ULA [8]. If the AoA of a UCA is limited to the azimuth plane, i.e. $\theta = \pi/2$, its array response can be expressed as [6], [10]:

$$G(f, \phi) = \sum_{m=-\infty}^{\infty} j^m J_m \left(2\pi f \frac{r}{c} \right) \exp(jm(\alpha_k - \phi)) \quad (6)$$

where J_n is the Bessel function of first kind and order m . The basis function $B(f, m)$ that produce a frequency invariant array response is defined as:

$$B(f, m) = \frac{1}{j^m J_m \left(2\pi f \frac{r}{c} \right)} \quad (7)$$

The element frequency response $H_i(f)$ can be transformed into the mode frequency response as [10]:

$$H(f, m) = \frac{1}{P} \sum_{i=0}^{P-1} H_i(f) B(f, m) \exp(-jm\phi_i) \quad (8)$$

Furthermore, the Bessel function has the following property [9]:

$$\left| J_{|m|} \left(2\pi f \frac{r}{c} \right) \right| \leq \left(\frac{2\pi f r e/c}{2|m|} \right)^{|m|} \quad (9)$$

This means that as m increases, the Bessel function approaches 0 and, consequently, the basis function $B(f, m)$ tends to ∞ . Therefore, only a limited number of modes can be included to calculate the basis function $B(f, m)$ so that it does not approach ∞ . The mode frequency response $H(f, m)$ can be transformed to the angular dependent frequency response using the IDFT:

$$\hat{H}(f, \phi) = \sum_{m=-\frac{M-1}{2}}^{\frac{M-1}{2}} H(f, m) \exp(jm\phi) \quad (10)$$

where M is the total number of modes used. Using the IDFT, the spatial channel impulse response using an invariant array response can be calculated:

$$\hat{h}(t, \phi) = \sum_{l=0}^{B/\Delta f} \hat{H}(f, \phi) \exp(j2\pi ft) \quad (11)$$

TABLE I
SIMULATION PARAMETERS

UCA elements	P	720
UCA radius r	r [m]	0.5
Central frequency	f_c [GHz]	28
Bandwidth	B [GHz]	2
Total frequency samples	Δf	750

TABLE II
MULTIPATH CHANNEL PARAMETERS

Path k	1	2	3	4	5	6	7	8
Delay τ_k [ns]	16	24	28	29	32	34	36	36
AoA α_k [deg]	0	0	180	55	-60	45	70	-50
Ampl [dB]	0	-3	-6	-6	-6	-15	-15	-20
Phase [deg]	0	45	-45	90	180	-90	135	-135

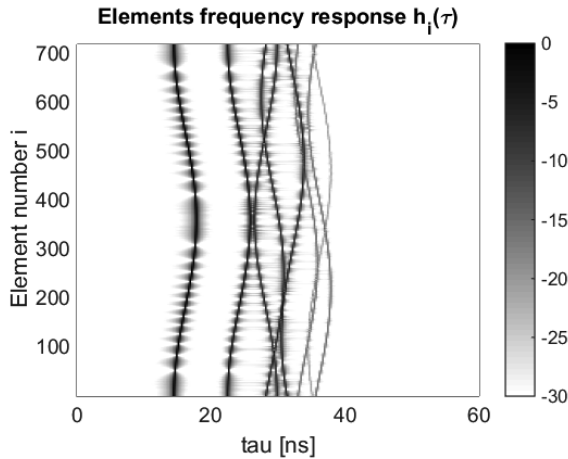


Fig. 2. Element-wise impulse response $h_i(\tau)$.

III. SIMULATION RESULTS

The parameters used in the simulation are summarized in Table I. The elements on the UCA are placed every half a degree and the separation between two consecutive elements is lower than half a wavelength at 29 GHz (the highest frequency considered) to avoid spatial aliasing. The bandwidth is selected to be 2 GHz, which results into a resolution of 0.5 ns in delay domain. For the simulation, a multipath channel with $K = 8$ paths is generated. The delay, AoA, amplitude and phase of the multipath components are shown in Table II.

Fig. 2 shows the element-wise impulse response obtained by applying the IDFT to (3). Let us take as an example the path with the lowest delay from Table II, i.e. $\tau_k = 16$. In the figure, we can see that the delay is around 16 ns, yet the delay for each element varies according to the relative delay given in (2) as expected. Furthermore, the delay of each antenna element varies according to the respective AoA and the array geometry as expected.

The response of the UCA given by (6) for different frequencies is shown on the left side of Fig. 3, whereas the frequency invariant response is shown on the right side. The UCA response varies over frequency as expected, while applying the basis function from (7) effectively converts the spatial response

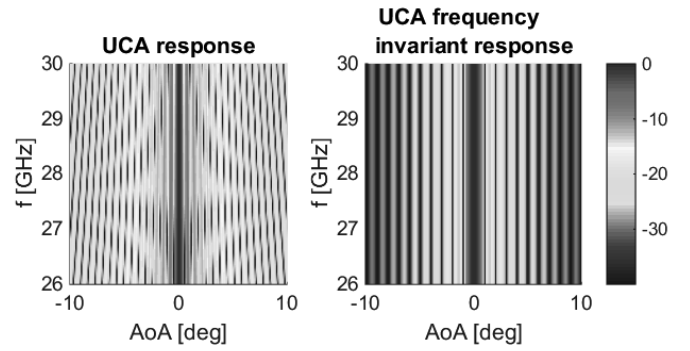


Fig. 3. UCA array response (left) and frequency invariant array response (right) across frequency.

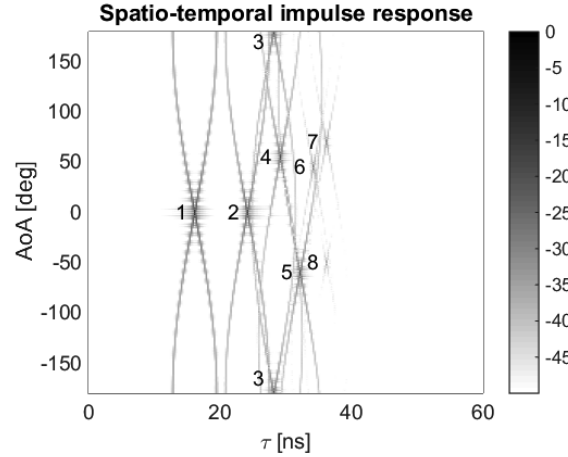


Fig. 4. Spatio-temporal channel impulse response from (5) using the classical beamforming approach.

from the UCA to a frequency invariant response.

Applying conventional beamforming as described in section II-A, the spatio-temporal channel impulse response from (5) is obtained and shown in Fig. 4. The path numbering from table II is used in the figure to facilitate the identification of the paths. High side lobes in both delay and angle domains can be observed due to the frequency dependent response of the UCA. Furthermore, some paths are almost not discernible due to the high sidelobes from stronger paths, e.g. paths 6 and 7. On the other hand, using the frequency invariant UCA response as described in section II-B reduces the side lobes considerably, as shown in Fig. 5.

Fig. 6 shows the power angular spectrum for both techniques. In this figure it is clear that weak paths, e.g. 6, 7, and 8, are buried by the high sidelobes from stronger paths. All paths are clearly visible using FIB. Moreover, the amplitude of the paths observed in Fig. 6 for the FIB technique fits perfectly with the initial path amplitudes given in table II.

IV. CONCLUSION AND FUTURE WORK

Accurate estimation of wideband channel parameters, e.g. delay and angle of the incoming multipath components, is important. In this paper, we discussed two beamforming techniques: one conventional beamforming technique that has been widely used for narrowband angle estimation, and a frequency

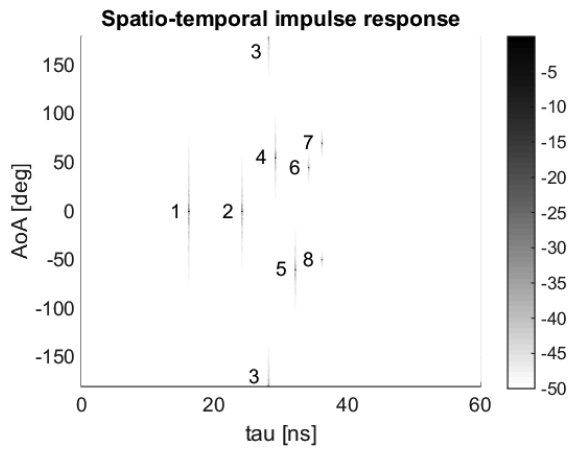


Fig. 5. Spatio-temporal channel impulse response from (11) using the FIB approach.

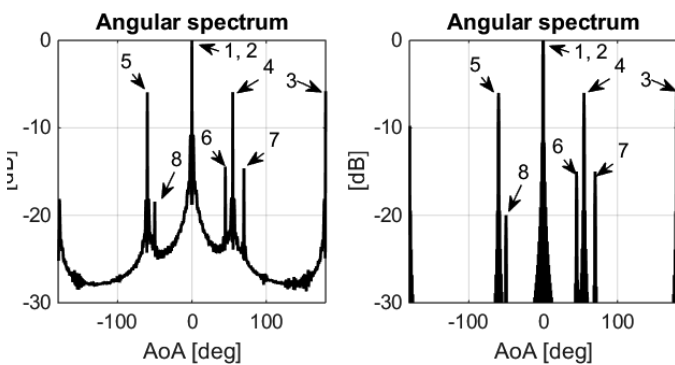


Fig. 6. Power angular spectrum using classical beamforming (left) and FIB (right).

invariant beamforming algorithm that could potentially be applicable to practical wideband mmWave measurements. The performance of the two algorithms were compared under a representative multipath channel. Simulation results showed that high joint sidelobes in delay and angle are present with the conventional beamforming algorithms and the weak paths could not be discerned from the estimated results. With the discussed frequency invariant beamformer, significant reduction on sidelobes is achieved and weak paths are recovered.

There are many logic extensions with the discussed frequency-invariant algorithms. In order to apply these algorithms to practical measurements, the impact of noise should be investigated. Furthermore, planar wavefronts are assumed in this investigation, yet this might not be the case in practical measurements. The last interaction point of the multipath components might be close to the array. Also the array size is generally large as well. The impact of spherical wavefronts should be investigated as well. In our study, we consider multipath components confined to a 2D plane, yet components with other elevation angles could appear in practice. In addition, different array structures could be investigated, e.g. planar array, or uniform concentric circular array.

ACKNOWLEDGMENT

This work has been supported by the Danish High Technology Foundation via the VIRTUOSO project.

REFERENCES

- [1] T. Rappaport, S. Sun, R. Mayzus, H. Zhao, Y. Azar, K. Wang, G. Wong, J. Schulz, M. Samimi, and F. Gutierrez, "Millimeter Wave Mobile Communications for 5G Cellular: It Will Work!" *Access, IEEE*, vol. 1, pp. 335–349, 2013.
- [2] J. Medbo, K. Borner, K. Haneda, V. Hovinen, T. Imai, J. Jarvelainen, T. Jamsa, A. Karttunen, K. Kusume, J. Kyrolainen, P. Kyosti, J. Meinila, V. Nurmela, L. Raschkowski, A. Roivainen, and J. Ylitalo, "Channel modelling for the fifth generation mobile communications," in *Antennas and Propagation (EuCAP), 2014 8th European Conference on*, April 2014, pp. 219–223.
- [3] J. Fuhl, J.-P. Rossi, and E. Bonek, "High-resolution 3-D direction-of-arrival determination for urban mobile radio," *Antennas and Propagation, IEEE Transactions on*, vol. 45, no. 4, pp. 672–682, Apr 1997.
- [4] P. Stoica and R. L. Moses, *Introduction to spectral analysis*. Prentice hall Upper Saddle River, 1997, vol. 1.
- [5] A. Kuchar, J.-P. Rossi, and E. Bonek, "Directional macro-cell channel characterization from urban measurements," *Antennas and Propagation, IEEE Transactions on*, vol. 48, no. 2, pp. 137–146, Feb 2000.
- [6] L. Parra, "Steerable frequency-invariant beamforming for arbitrary arrays," *IEEE Workshop on Applications of Signal Processing to Audio and Acoustics*, pp. 102–105, October 2005.
- [7] M. Wax and J. Sheinvald, "Direction finding of coherent signals via spatial smoothing for uniform circular arrays," *IEEE Transactions on Antennas and Propagation*, vol. 42, 1994.
- [8] S. Takashi and Y. Karasawa, "Wideband beamspace adaptive array utilizing FIR fan filters for multibeam forming," *IEEE Transactions on Signal Processing*, vol. 48, 2000.
- [9] S. Chan and H. Chen, "Uniform concentric circular arrays with frequency-invariant characteristics - theory, design, adaptive beamforming and doa estimation," *IEEE Transactions on Signal Processing*, vol. 55, 2007.
- [10] C. Gentile, A. J. Braga, and A. Kik, "A comprehensive evaluation of joint range and angle estimation in ultra-wideband systems for indoors," *IEEE International Conference on Communications, (ICC '08)*, pp. 4219–4225, May 2008.